

# Resonances as Probes of Heavy-Ion Collisions at ALICE

**A. G. Knospe (for the ALICE Collaboration)**

The University of Texas at Austin, Department of Physics, Austin, TX, USA

E-mail: `anders.knospe@cern.ch`

**Abstract.** Hadronic resonances serve as unique probes in the study of the hot and dense nuclear matter produced in heavy-ion collisions. Properties of the hadronic phase of the collision can be extracted from measurements of the suppression of resonance yields. A comparison of the transverse-momentum spectra of the  $\phi(1020)$  meson and the proton (which have similar masses) can be used to study particle production mechanisms. Resonance measurements in pp collisions provide input for tuning QCD-inspired particle production models and serve as reference measurements for other collision systems. Measurements of resonances in p-Pb collisions allow nuclear effects in the absence of a hot and dense final state to be studied. The ALICE Collaboration has measured resonances in pp, p-Pb, and Pb-Pb collisions. These measurements will be discussed and compared to results from other experiments and to theoretical models.

Resonances serve as useful probes that allow the characteristics of heavy-ion collisions to be studied at different stages of their evolution. While the yields of stable hadrons are fixed at chemical freeze-out, the yields of resonances can be modified by hadronic scattering processes after chemical freeze-out [1–3]. Regeneration, in which resonance decay products scatter pseudo-elastically through a resonance state (*e.g.*,  $\pi K \rightarrow K^{*0} \rightarrow \pi K$ ), can increase the measured yield of the intermediate resonance state without changing the yields of the stable hadrons. Elastic re-scattering of a resonance decay product can smear the invariant mass resolution and may impede reconstruction of the original resonance. Pseudo-elastic scattering of a resonance decay product through a different resonance state (*e.g.*, a pion from a  $K^{*0}$  decay scattering through a  $\rho$  state) will prevent reconstruction of the first resonance [4]. Regeneration and re-scattering are expected to be most important for  $p_T \lesssim 2$  GeV/c [1, 4]. The final resonance yields at kinetic freeze-out will be determined by the chemical freeze-out temperature, the time between chemical and kinetic freeze-out, the resonance lifetime, and the scattering cross sections of its decay products with other hadrons. Theoretical models that take these effects into account can be used to estimate the properties of the hadronic phase using measured resonance yields (or their ratios to stable particles) as input [2, 5, 6].

In addition, partial restoration of chiral symmetry around the phase transition between partonic and hadronic matter may lead to changes in the masses or the widths of resonances [7–10]. Mechanisms that determine the shapes of particle  $p_T$  spectra, including the relative strengths of quark recombination [11, 12] and hydrodynamical effects [13–15], are studied experimentally using many different particle species; the  $\phi(1020)$ , a meson with a mass similar to the proton, provides valuable information regarding the effects of mass and baryon number on the shapes of particle  $p_T$  spectra. Measurements of the nuclear modification factor  $R_{AA}$  of hadrons allows the in-medium energy loss of partons to be studied. Resonance  $R_{AA}$  measurements will

provide constraints against which the results of theoretical models can be tested. The effects of ordinary nuclear matter on particle  $p_T$  spectra can be studied through measurement of the nuclear modification factor in p–Pb collisions ( $R_{pPb}$ ).

These proceedings describe recent results from the ALICE experiment related to these topics, with the focus on the  $K^{*0}$  (denoting the average of  $K^*(892)^0$  and  $\bar{K}^*(892)^0$ ) and the  $\phi$  (abbreviating  $\phi(1020)$ ). Further details of these results can be found in [16–19]. The main components of the ALICE detector [20] used in the analyses described here are the Inner Tracking System (for tracking and vertex finding), Time Projection Chamber [21] (for tracking and particle identification), the Time-of-Flight detector (for particle identification), and the VZERO detector (used to determine event multiplicity and centrality classes).

The  $K^{*0}$  and  $\phi$  are measured through invariant-mass reconstruction of their charged hadronic decay channels ( $K^{*0} \rightarrow \pi^\pm K^\mp$  and  $\phi \rightarrow K^- K^+$ ). The combinatorial background is estimated using an event-mixing technique. After subtraction of this background, the resonance signals are fitted using a peak fit function (a relativistic Breit-Wigner function for  $K^{*0}$ , the convolution of a Breit-Wigner function and a Gaussian for  $\phi$ ) added to a first- or second-order polynomial, which describes the residual background. The  $p_T$ -dependent yields, masses, and widths of  $K^{*0}$  and  $\phi$  are extracted from these fits. The  $p_T$  spectra are fitted using Lévy-Tsallis functions for pp and p–Pb collisions and Boltzmann-Gibbs blast-wave functions for Pb–Pb collisions. These fit functions are used to extract the mean transverse momentum  $\langle p_T \rangle$  and to extrapolate the resonance yields below the lowest measured  $p_T$  bin so that the total  $p_T$ -integrated yield can be calculated. These quantities have been measured for Pb–Pb collisions at  $\sqrt{s_{NN}} = 2.76$  TeV [18], p–Pb collisions at  $\sqrt{s_{NN}} = 5.02$  TeV [19], and pp collisions at  $\sqrt{s} = 0.9, 2.76,$  and  $7$  TeV [16, 17, 19].

The  $K^{*0}$  and  $\phi$  masses and widths have been measured as functions of  $p_T$  for central and peripheral Pb–Pb collisions at  $\sqrt{s_{NN}} = 2.76$  TeV [18]. These quantities are consistent with the values extracted from Monte-Carlo simulations (in which particles are produced using HIJING and their interactions with the ALICE detector are simulated using GEANT3) and no centrality dependence is observed.

The ratios of  $p_T$ -integrated particle yields  $K^{*0}/K$  and  $\phi/K$  are shown in Fig. 1(a) as a function of  $(dN_{ch}/d\eta)^{1/3}$  for pp, p–Pb, and Pb–Pb collisions. The abscissa  $(dN_{ch}/d\eta)^{1/3}$  is used as a proxy for the system radius, following a practice used in femtoscopy studies [22]. The  $K^{*0}/K^-$  ratio in central collisions is suppressed with respect to the ratio in pp, p–Pb, and peripheral Pb–Pb collisions. The  $K^{*0}/K^-$  ratio is also suppressed with respect to the value extracted from a thermal model fit of ALICE data [23] with a chemical freeze-out temperature of 156 MeV and zero baryo-chemical potential (the  $K^{*0}$  is excluded from this fit). The centrality-dependent suppression of the  $K^{*0}/K^-$  ratio in Pb–Pb collisions is consistent with a scenario in which the reconstructible  $K^{*0}$  yield is reduced due to re-scattering (with re-scattering being stronger than regeneration). As described in [18], the measured  $K^{*0}/K^-$  ratio in central Pb–Pb collisions can be used along with a theoretical model [2, 5, 6] (a thermal model with resonance yields modified by re-scattering) to obtain an estimate of 2 fm/c for the lower limit of the time between chemical and kinetic freeze-out. In contrast, the  $\phi/K$  ratio is not suppressed in central collisions and only a weak centrality dependence is observed. This suggests that re-scattering effects are not important for the  $\phi$ , which has a lifetime an order of magnitude longer than the  $K^{*0}$  and longer than many estimates of the lifetime of the hadronic phase. The  $K^{*0}/K$  and  $\phi/K$  ratios measured in p–Pb collisions are consistent with the trends observed in pp and peripheral Pb–Pb collisions. The  $K^{*0}/K^-$  ratios measured in pp and A–A collisions at  $\sqrt{s_{NN}} = 62.4$  and 200 GeV [24] follow the same trend as the values observed at LHC energies. The  $\phi/K^-$  ratios observed in pp, d–Au, and A–A collisions at  $\sqrt{s_{NN}} = 200$  GeV [25] are consistent within uncertainties with the values observed at the LHC for similar values of  $(dN_{ch}/d\eta)^{1/3}$ , although the RHIC measurements tend to be larger than the values observed at LHC.

The  $p/\pi$  ratio shows a pronounced increase as a function of  $p_T$  for  $p_T < 3$  GeV/c in Pb–Pb

collisions [26]. Different explanations have been proposed as the cause of this increase. An increasing baryon-to-meson ratio in this  $p_T$  range suggests quark recombination as the particle production mechanism. However, hydrodynamical effects could also lead to an increasing  $p/\pi$  ratio because of the different masses of the two particles. The  $\phi$ , a meson that has a mass similar to the proton (within 9%), allows the baryon-to-meson ratio to be studied without the added complication of a mass difference. Fig. 1(b) shows the  $p/\phi$  ratio as a function of  $p_T$  for different centrality and multiplicity intervals in pp, p-Pb, and Pb-Pb collisions [19]. For central Pb-Pb collisions, the ratio is flat for  $p_T < 3 - 4$  GeV/c. This is consistent with hydrodynamical effects: the shapes of the  $p_T$  spectra are determined by the particle masses and not the quark content. In peripheral Pb-Pb collisions, the  $p/\phi$  ratio takes on an increasingly steep slope, suggesting that the p and  $\phi$  may have different production mechanisms in these collisions. The values and slopes of the  $p/\phi$  ratio observed in pp and low-multiplicity p-Pb collisions are similar to those observed in peripheral Pb-Pb collisions. The  $p/\phi$  ratio in p-Pb collisions does not depend on multiplicity for  $p_T > 1$  GeV/c. A possible flattening in this ratio is observed for  $p_T < 1$  for high-multiplicity p-Pb collisions, which could be interpreted as a hint for the onset of collective behavior in these collisions.

The mean transverse momentum  $\langle p_T \rangle$  has been measured for  $\pi^\pm$ ,  $K^\pm$ , (anti)protons,  $K^{*0}$ , and  $\phi$  in pp, p-Pb, and Pb-Pb collisions and for  $\Lambda$  in p-Pb collisions [17–19, 26, 27]. Mass ordering in  $\langle p_T \rangle$  is observed in central Pb-Pb collisions. The  $K^{*0}$ , p, and  $\phi$ , which have similar masses, are observed to have similar  $\langle p_T \rangle$  values. This is expected from hydrodynamical models. However, a splitting is observed between the p and  $\phi$  for peripheral Pb-Pb collisions, with the  $\phi$  having large  $\langle p_T \rangle$  values. The same effect is observed in the  $p/\phi$  ratio. In p-Pb and pp collisions, the mass ordering is only approximate:  $\langle p_T \rangle$  for the resonances is larger than  $\langle p_T \rangle$  for p and  $\Lambda$ . A plot of  $\langle p_T \rangle$  as a function of particle mass suggests the possibility of two different trends: one for the mesons (including the resonances) and another for the baryons. The values of  $\langle p_T \rangle$  for p-Pb follow different trends from the values for Pb-Pb collisions as functions of  $(dN_{\text{ch}}/d\eta)^{1/3}$  [19]. The values of  $\langle p_T \rangle$  for the highest-multiplicity p-Pb collisions reach (or even exceed) the values observed for central Pb-Pb collisions, despite originating from a smaller system. This suggests the possibility of different particle production mechanisms in Pb-Pb and p-Pb collisions.

The nuclear modification factors of these resonances have been computed for Pb-Pb collisions at  $\sqrt{s_{\text{NN}}} = 2.76$  TeV ( $R_{\text{AA}}$ ) and p-Pb collisions at  $\sqrt{s_{\text{NN}}} = 5.02$  TeV ( $R_{\text{pPb}}$ , for  $\phi$  only) [19]. For central Pb-Pb collisions at high  $p_T$  ( $\gtrsim 5$  GeV/c), both  $K^{*0}$  and  $\phi$  are strongly suppressed ( $R_{\text{AA}} \approx 0.15 - 0.2$ ), with similar suppression observed for charged hadrons and identified  $\pi^\pm$ ,  $K^\pm$ , and p. At low  $p_T$  ( $< 2$  GeV/c), the  $K^{*0}$  is more suppressed than charged hadrons in central Pb-Pb collisions, which may be an indication that re-scattering effects are of greater importance in this  $p_T$  range. For  $2 < p_T < 6$  GeV/c in central collisions, the  $\phi$   $R_{\text{AA}}$  is greater than  $R_{\text{AA}}$  for the lighter mesons ( $\pi^\pm$  and  $K^\pm$ ), but less than  $R_{\text{AA}}$  for protons, which have a similar mass. Since no pp reference  $p_T$  spectra have yet been measured at  $\sqrt{s} = 5.02$  TeV, the reference for  $R_{\text{pPb}}$  is calculated by interpolating between measured  $\phi$  spectra for  $\sqrt{s_{\text{NN}}} = 2.76$  and 7 TeV. The values of  $R_{\text{pPb}}$  for  $\phi$  indicate a moderate Cronin peak (reaching a value of  $\approx 1.2$ ) for  $3 < p_T < 6$  GeV/c. In contrast,  $\pi^\pm$  have no significant Cronin peak, while protons appear to have a stronger Cronin peak in the same  $p_T$  range. For  $p_T \gtrsim 8$  GeV/c,  $R_{\text{pPb}}$  does not deviate from unity for  $\pi^\pm$ , p, or  $\phi$ .

In summary, the  $K^{*0}$  and  $\phi$  resonance have been measured in different collision systems at LHC energies. The  $K^{*0}/K$  ratio is suppressed in central collisions, consistent with re-scattering of its decay daughters, while the  $\phi/K$  ratio is not suppressed due to its longer lifetime. The  $\phi/p$  ratio is flat for  $p_T < 3 - 4$  GeV/c in central Pb-Pb collisions, which is expected from hydrodynamical models since the particles have similar masses. The values of  $\langle p_T \rangle$  in Pb-Pb and p-Pb collisions follow different trends as a function of  $(dN_{\text{ch}}/d\eta)^{1/3}$  and strict mass ordering of  $\langle p_T \rangle$  values is violated for  $K^{*0}$ , p,  $\phi$ , and  $\Lambda$  in p-Pb collisions. The nuclear modification factor

$R_{AA}$  of resonances at high  $p_T$  shows large suppression, consistent with the suppression observed for stable hadrons. At high  $p_T$ , the  $\phi$  meson  $R_{pPb}$  is consistent with unity.

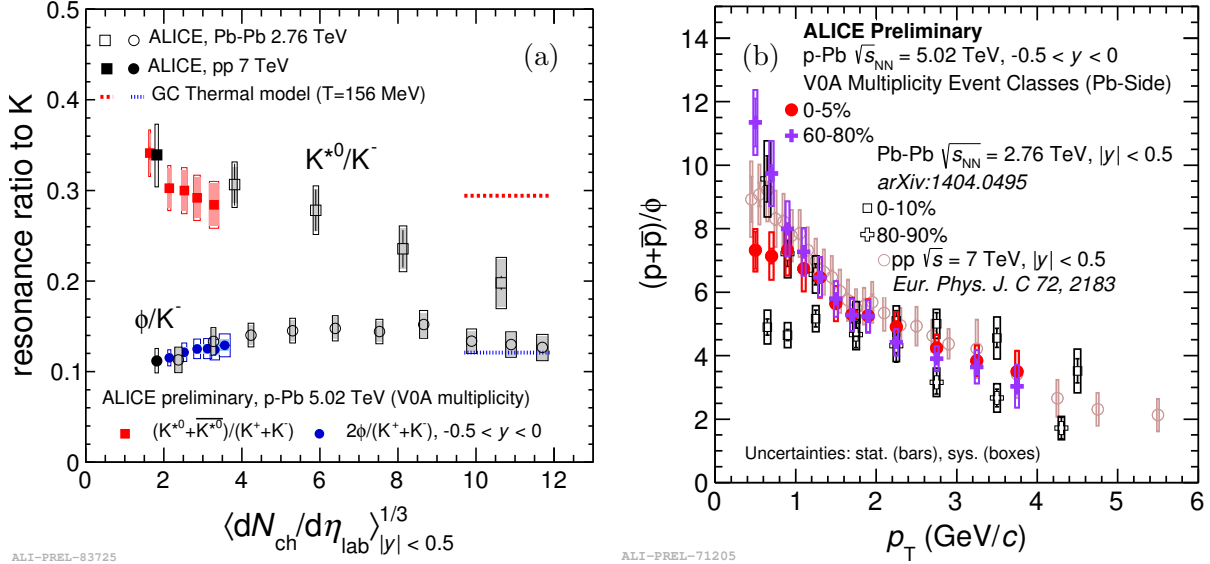


**Figure 1.** For pp, p-Pb, and Pb-Pb collisions: (a) ratios  $K^{*0}/K$  and  $\phi/K$  as functions of  $(dN_{ch}/d\eta)^{1/3}$ , (b): Ratio  $p/\phi$  as a function of  $p_T$  in different centrality and multiplicity intervals.

## References

- [1] Bleicher M and Stöcker H 2004 *J. Phys. G* **30** S111–8
- [2] Markert C *et al* 2002 *Proc. of PASI 2002* ed Elze H T *et al* pp 533–52 (Preprint arXiv:hep-ph/0206260)
- [3] Vogel S and Bleicher M 2005 *Proc. of the 43rd International Winter Meeting on Nuclear Physics, Bormio, Italy, 2005* ed Iori I and Moroni A (INSPIRE) (Preprint arXiv:nucl-th/0505027)
- [4] Bleicher M and Aichelin J 2002 *Phys. Lett. B* **530** 81–87
- [5] Torrieri G and Rafelski J 2001 *Phys. Lett. B* **509** 239–45
- [6] Rafelski J, Letessier J and Torrieri G 2001 *Phys. Rev. C* **64** 054907
- [7] Brown G E and Rho M 2002 *Rhys. Rep.* **363** 85–171
- [8] Rapp R *et al* 2010 *Relativistic Heavy Ion Physics* ed Stock R (Springer Berlin Heidelberg) pp 134–75
- [9] Brodsky S J and de Teramond G F 1988 *Phys. Rev. Lett.* **60** 1924–7
- [10] Eletsky V L, Belkacem M, Ellis P J and Kapusta J I 2001 *Phys. Rev. C* **64** 035202
- [11] Fries R, Muller B, Nonaka C and Bass S 2003 *Phys. Rev. Lett.* **90** 202303
- [12] Fries R, Greco V and Sorensen P 2008 *Annu. Rev. Nucl. Part. Sci.* **58** 177–205
- [13] Qui Z, Shen C and Heinz U 2012 *Phys. Lett. B* **707** 151–5
- [14] Shen C, Heinz U, Huovinen P and Song H 2011 *Phys. Rev. C* **84** 044903
- [15] Bożek P and Wyskiel-Piekarska I 2012 *Phys. Rev. C* **85** 064915
- [16] Aamodt K *et al* (ALICE Collaboration) 2011 *Eur. Phys. J. C* **71** 1594
- [17] Abelev B *et al* (ALICE Collaboration) 2012 *Eur. Phys. J. C* **72** 2183
- [18] Abelev B *et al* (ALICE Collaboration) 2014 *CERN-PH-EP-2014-060* (Preprint arXiv:1404.0495)
- [19] Bellini F (for the ALICE Collaboration) 2014 *Nucl. Phys. A* **931** 846–50
- [20] Aamodt K *et al* (ALICE Collaboration) 2008 *J. Inst.* **3** No. S08002 i–245
- [21] Alme J *et al* 2010 *Nucl. Inst. Meth. in Phys. Res. A* **622** 316–67
- [22] Lisa M A *et al* 2005 *Annu. Rev. Nucl. Part. Sci.* **55** 357
- [23] Stachel J, Andronic A, Braun-Munzinger P and Redlich K 2014 *J. Phys.: Conf. Ser.* **509** 012019
- [24] Aggarwal M M *et al* (STAR Collaboration) 2011 *Phys. Rev. C* **84**(3) 034909
- [25] Abelev B I *et al* (STAR Collaboration) 2009 *Phys. Rev. C* **79** 064903
- [26] Abelev B *et al* (ALICE Collaboration) 2013 *Phys. Rev. C* **88** 044910
- [27] Abelev B *et al* (ALICE Collaboration) 2014 *Phys. Lett. B* **728** 25–38